

Investigating the Mechanism of a Common Genetic Variant Associated with Human Cortical Surface Area

By
Grace Morningstar

Senior Honors Thesis
Biology
University of North Carolina at Chapel Hill
03/20/2020

Approved:

Thesis Advisor

Reader

Reader

Abstract

The surface area of the modern human cerebral cortex has greatly expanded along our evolutionary lineage (Rakic, 2000). Of the intercellular messages that have been found to impact embryonic development, Wnt proteins have been shown to be integral drivers of human cortical development and expansion (Chenn, 2008). It remains unclear if human genetic variation within genes of the Wnt family leads to differences in Wnt signaling activity, and whether altered Wnt signaling levels ultimately lead to differences in human cortical structure (Kwan, 2016). In this study, we sought to understand whether a common genetic variant in *WNT2B* significantly associated with decreased cortical surface area through Genome-Wide Association Study (GWAS) impacted Wnt signaling activity in HEK293 and hNP cell lines. In order to answer this question, we used dual-luciferase technology upon whole-plasmid transient transfection of human embryonic kidney (HEK293) and human neural progenitor (hNP) cells. We found that there was differential activation between the surface area-increasing allele and the surface area-decreasing allele of *WNT2B* in HEK293 cells, and a largely irreproducible difference in Wnt activation levels between the alleles in hNP cells. These results indicate that the variant impacts Wnt activation in human embryonic kidney tissue, but other methods can and should be used in human neural progenitors to obtain trustworthy results.

Introduction

Neural development at a glance is fairly intuitive: as our bodies grow and mature, our brains follow suit, in both size and cognitive faculties. Apart from a general increase in cortical size, arguably the most significant process that occurs during neural development is the drastic increase in surface area produced through cortical folding. It is humans' vast cortical surface area that distinguishes our brains most prominently from those of other animals (Grasby, 2019). In the same vein, we hypothesize that humans' expansive cortical surface area is what enables our higher cognitive faculties (Grasby, 2019). According to the radial unit hypothesis, the increase in adult cortical surface is a result of proliferation dynamics of cells found in the ventricular zone during fetal development (Rakic, 2000). These progenitor cells migrate upward and differentiate before settling in the outer cortical plate. Progenitor cells proliferate and migrate in units called radial columns; essentially, this model states that the more radial columns present, the greater the surface area produced. Abnormal development of cortical structure has long been thought to play a role in human diseases such as schizophrenia and autism spectrum disorder (Kwan, 2016, Hoseth, 2018).

How does common genetic variation, in the form of single nucleotide polymorphisms (SNPs), impact how the cortex is shaped? Single nucleotide polymorphisms are regions within the genome where there is single nucleotide variation between individuals. A Genome-Wide Association Study (GWAS) was conducted with the goal of identifying SNPs associated with

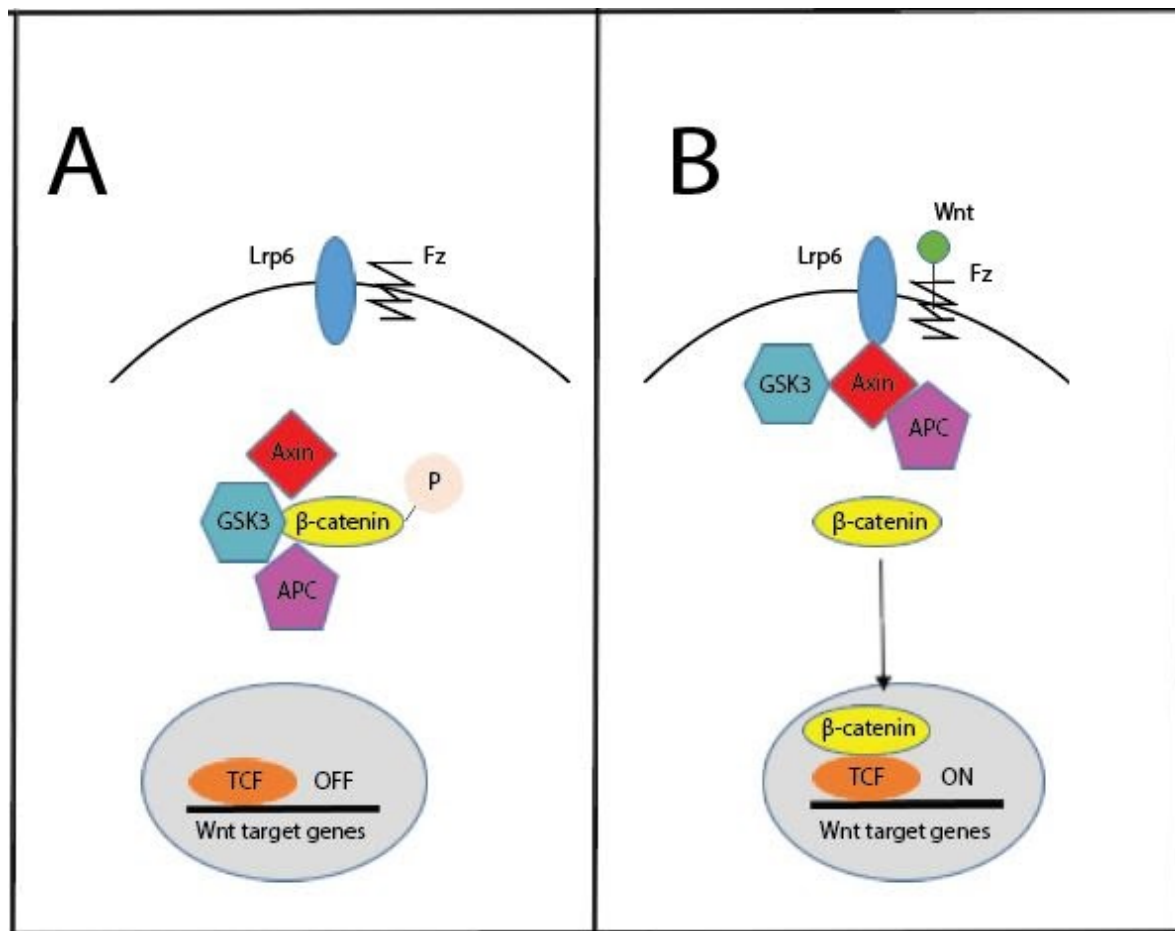
cortical surface area development (Stein et al., 2014). A SNP within *WNT2B* was identified through this GWAS, which implicated its involvement in the surface area development of the lingual gyrus (Stein et al., 2014). The reference allele of *WNT2B* is associated with increased surface area of the lingual gyrus, and the alternative allele of *WNT2B* is associated with decreased surface area of the same region.

Wnt proteins constitute a superfamily of secreted, locally-acting proteins that have been implicated in the proliferation and physical arrangement of multiple cell types (Nusse, 2019). Due to the wide-reaching implications of cell proliferation in development, Wnt proteins are known to play a role in numerous human diseases, including autism (Kwan, 2016). Wnt proteins have been studied extensively in cell types associated with cancer, overarchingly in terms of their role in determining physical axes during embryonic development, and also in the context of their role in neural development (Kwan, 2016). Despite how widely studied Wnt signaling has been, very little research has been conducted regarding how *WNT2B* may impact neural development at any stage. By examining how the variant alters Wnt activation, we can gain some insight into how the variant may impact the development of human cortical surface area.

To discover the mechanism through which this GWAS-supported variant within *WNT2B* impacts cortical structure, we obtained plasmids containing the reference *WNT2B* allele. After executing site-directed mutagenesis on the reference plasmid to induce the SNP-associated point mutation and create the surface area-decreasing *WNT2B* allele, first HEK293 and then hNP cells were transfected with each plasmid. In addition, cells were transfected with Wnt-specific and

nonspecific luciferase reporters in order to find Wnt activation levels using luminescence detection (Biechele, 2008). Our luciferase constructs, BAR and Renilla luciferase, utilize the luciferase gene (derived from fireflies or a variety of sea pansy) fused to a Beta catenin-activated receptor gene and a nonspecific promoter, respectively (Biechele, 2008). The dual-luciferase reporters serve to indicate activation of the Wnt pathway as well as background cellular activity for normalization. We found that there was significant differential activation of the Wnt pathway between cells transfected with the surface area-increasing and surface area-decreasing alleles in HEK293 cells. In hNP cells, there was largely irreproducible and insignificant Wnt activation in hNP cells transfected with the surface area-decreasing allele compared to the surface area-increasing allele, as well as inconsistent positive control activation.

Figure 1. Simplified diagram of canonical Wnt signaling pathway.



Simplified diagram of Wnt signaling pathway. In the absence of Wnt ligand, Beta-catenin is targeted for degradation by a protein complex consisting of axin, GSK3, and APC. In the presence of Wnt ligand, Wnt protein binds to transmembrane receptor Fz, which initiates a signaling cascade that frees Beta-catenin from degradation. Beta-catenin then enters the nucleus and binds to transcription factor TCF. TCF then drives transcription of Wnt target genes.

Methods

Genetic Targeting

We used the ENIGMA GWAS data (Stein et al., 2014), as well as the University of California-Santa Cruz Genome Browser, to learn more about the characteristics of the implicated SNP in *WNT2B*. The SNP is identified as rs910697, and indicates a point mutation at the codon level from A to G. According to the GWAS results, the A allele is associated with increased cortical surface area of the lingual gyrus, while the G allele is associated with decreased cortical surface area of the lingual gyrus. The codon affected by this SNP is CAA, which codes for glutamine. The SNP changes the third-position A to G, resulting in a synonymous mutation that, by definition, causes no shift in the gene's amino acid sequence. The Wnt plasmid sequences were visualized using SnapGene software. Reference *WNT2B* plasmids (Addgene, ID: 35907) were obtained through Addgene.org from the Marian Waterman Lab. The alternative *WNT2B* gene was created through site-directed mutagenesis conducted on this reference stock.

Cell Culture

HEK293 cells were cultured in DMEM-high glucose (ThermoFisher, 11965092) with 10% fetal bovine serum (FBS) (Gibco, Cat: 16000036).

Human neural progenitor cell samples were obtained from the University of California at Los Angeles (Stein et al, 2014). 500 mL of Neurobasal A media (Life Technologies, Cat: 10888-022)

was supplemented with primocin (Invivogen, Cat: ant-pm-2) diluted 1:500, BIT serum substitute (Stemcell Technologies, Cat: 09500) diluted 3:25, Glutamax (100x) (Life Technologies, Cat: 35050-061) diluted 1:100, 10mg/mL heparin (Sigma-Aldrich, Cat: H3393-10KU) diluted 1:10,000. Full-feeds, consisting of EGF (Life Technologies, Cat: PHG0313) and FGF (Life Technologies, Cat: PHG0023), LIF (Life Technologies, Cat: PHC9481), and PDGF (Life Technologies, Cat: PHG0134) all diluted 1:5000 in enough media to completely replenish all wells ($100\mu\text{L}/320\text{mm}^2$), were administered for the first week after sample thawing. Half-feeds were administered for the remainder of the cells' time *in vitro*, and consisted of enough neurobasal A media to replace half of the media within each well ($50\mu\text{L}/320\text{mm}^2$), and twice the amount of EGF/FGF, LIF, and PDGF that would be used for a full feed (diluted 1:2500). Prior to cell plating, 96-well plates were administered two coats 24 hours apart. Recipe for 1st coat per 10cm dish: 5mL PBS and $10\mu\text{L}/\text{mL}$ 100x poly-ornatine (Sigma-Aldrich, Cat: P3655-500MG). Recipe for 2nd coat per 10cm² dish: 5ml PBS and fibronectin diluted 1:200 (Sigma-Aldrich, Cat: F4759).

Mutagenesis

50 ng of template plasmid DNA was mixed with $2.5\mu\text{L}$ of Pfu buffer (Promega, Cat: 9PIM774), $1\mu\text{L}$ primer, $0.5\mu\text{L}$ dNTPs, $0.2\mu\text{L}$ PFU DNA Polymerase Turbo (Agilent Technologies, Cat: 600250), and $20\mu\text{L}$ molecular-grade water. PCR was completed using a thermal cycler, using the protocol 1' at 95°C , 1' at 55°C , and 1'/kb at 68°C . $20\mu\text{L}$ of the PCR reaction was then added to a new microcentrifuge tube, and $1\mu\text{L}$ of DpnI (New England Biolabs, Cat: R0176S) was added and

mixed thoroughly. After one hour of incubation at 37°C, competent E.coli cells (Invitrogen, Cat: 18265017) were thawed on ice, and 25µL of E.coli cells were placed into PCR tubes. 1µL of each PCR reaction was added to each tube of competent cells, then heat-shocked for 30 seconds at 42°C in a circulating water bath. 100µL of S.O.C. medium (Invitrogen, Cat: 15544034) was then added, and the mixture was shaken for one hour at 37°C. 7µL of the mixture were then added to ampicillin plates divided into quarters and labeled for the conditions: -taq/-DpnI, +taq/-DpnI, -taq/+DpnI, +taq/+DpnI. Colonies selected from the +taq/+DpnI condition were cloned, mini-prepped using the QIAGEN mini-prep kit (Cat: 27104), and Sanger sequenced to ascertain whether they contained the desired DNA sequences.

Transient Transfection

HEK293 cells were plated at 3×10^4 cells/320mm² and transfected with 10µL of FuGENE (ProMega, Cat: E2311), 100 ng of BAR, 50 ng Renilla, 100ng Wnt plasmid, and 1µL of 2000ng/µL GFP. Concentrations of Wnt plasmids, control plasmids, and luciferase reporter constructs varied depending on mini-prep. All concentrations were between 150 and 2000ng/µL.

hNPs were plated at 1.5×10^4 cells/320mm². For hNPs, the ThermoFisher Lipofectamine Stem Reagent (STEM00003, Cat: 4002) protocol was used. Per each well in a 24-well plate, one microcentrifuge tube contained 1 µL of Lipofectamine Stem reagent diluted in 25 µL of Opti-MEM I medium (Gibco, Cat: 31985070). Another tube contained 500 ng of DNA, including GFP, BAR and Renilla plasmids, and Wnt overexpression plasmid, diluted in 25 µL of

Opti-MEM I medium. The two tubes were combined, mixed thoroughly, and incubated at room temperature for 10 minutes. 50 μ L of the mixture were then added to each desired well, and allowed to incubate at 37°C for 24 hours. In order to tailor the protocol to the wells of a 96-well plate, lipofectamine and overall mixture volumes were proportionally adjusted (0.3 μ L of lipofectamine and 30 μ L of lipofectamine/DNA mixture per 320mm²) .

All fluorescence from GFP was visualized using fluorescent microscopy, and was used to determine transfection efficiency, with a desired efficiency of at least 35%.

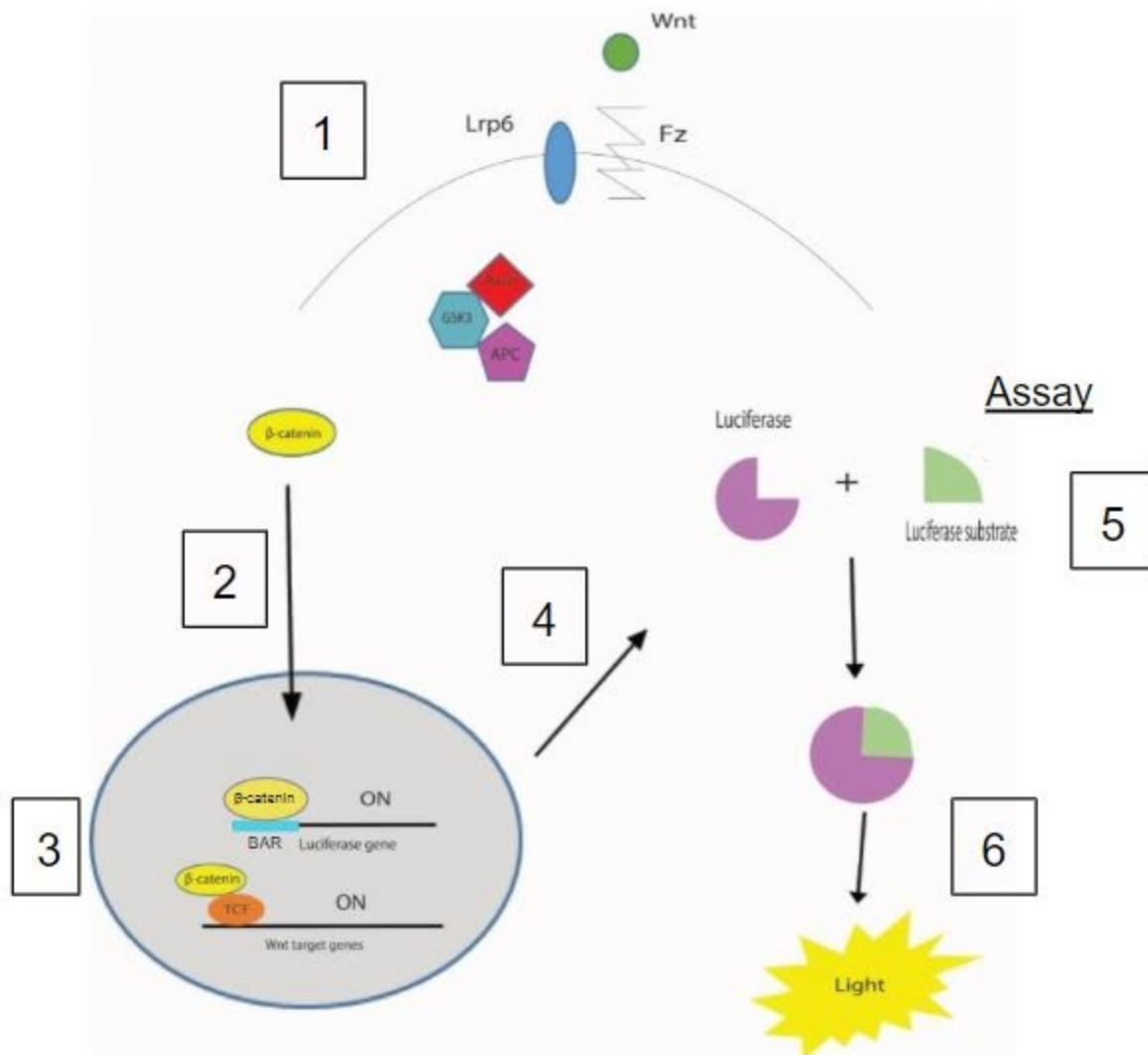
Transfection Condition	Overexpression Plasmid Used
Negative Control	No overexpression plasmid
Positive control	Ube3a (HEK293)
Surface area-increasing allele	Wnt2b_rs910697_[A]
Surface area-decreasing allele	Wnt2b_rs910697_[G]

Luciferase Assay and Computational Analysis

After removing all media, 35 μ L of 1x passive lysis buffer (Cat: E1941) was added to each transfected well. 33 μ L of lysate was transferred to a solid 384-well plate. 38 μ L of Luciferase substrate (Cat: E151A of E1910) diluted 1:50 in Luciferase buffer (Cat: E195A of E2920) was added to lysate-containing wells. The plate was centrifuged for 15-20 seconds, then shaken for additional reagent dispersal, and read in the GloMax plate reader, using GloMax luminescence

software. 38 μ L of Stop & Glo substrate (Promega, Cat: E313A) diluted 1:100 in Stop & Glo buffer (Promega, Cat: E298A) was then added to the wells. The plate was centrifuged for 15-20 seconds, then shaken and read in the GloMax plate reader. Data was plotted and two-tailed t-test was run using Microsoft Excel and Rstudio. Four replicates were included in each condition, and the same donor was used across all transfected plates.

Figure 2. Mechanism of BAR Luciferase



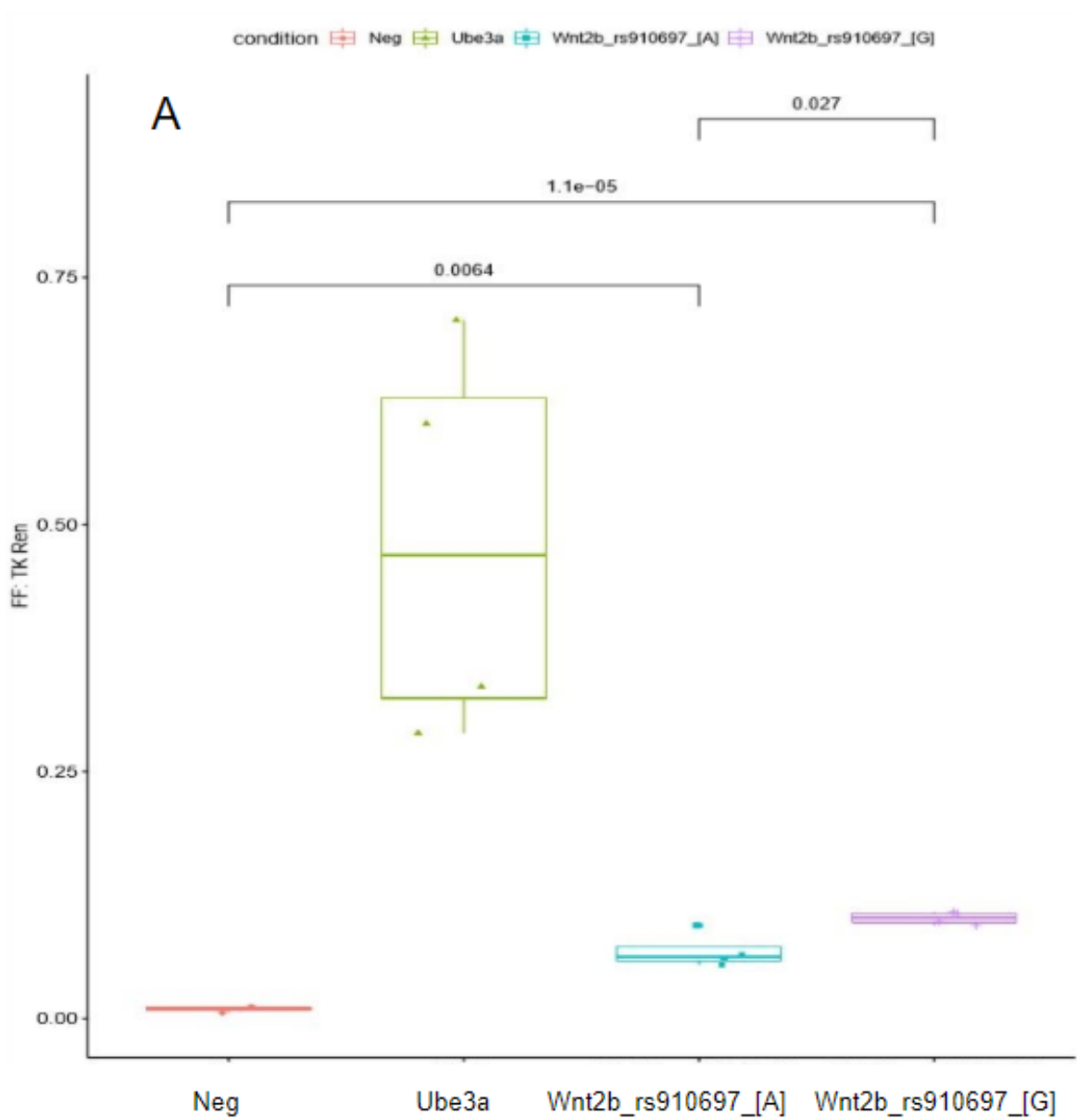
Simplified diagram of BAR luciferase mechanism of action. After entering the nucleus, BAR is activated by Beta-catenin, which drives transcription of the luciferase (FIREFLY) gene. After cells are lysed, luciferase substrate is added to the cells, which binds to the luciferase protein, and produces luminescence. Renilla works similarly, but operates under a general promoter that is not specifically activated by Wnt pathway proteins.

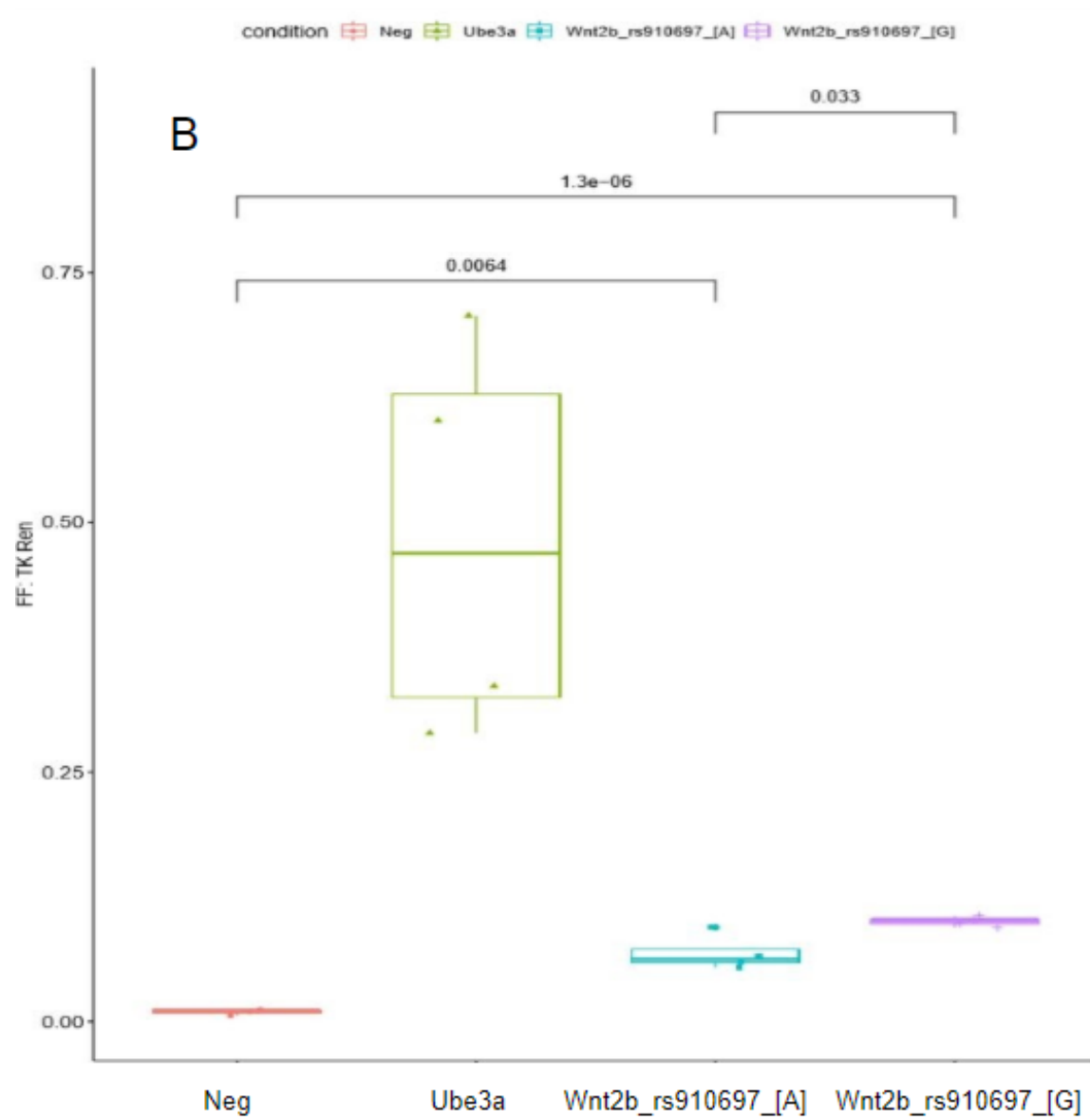
Results

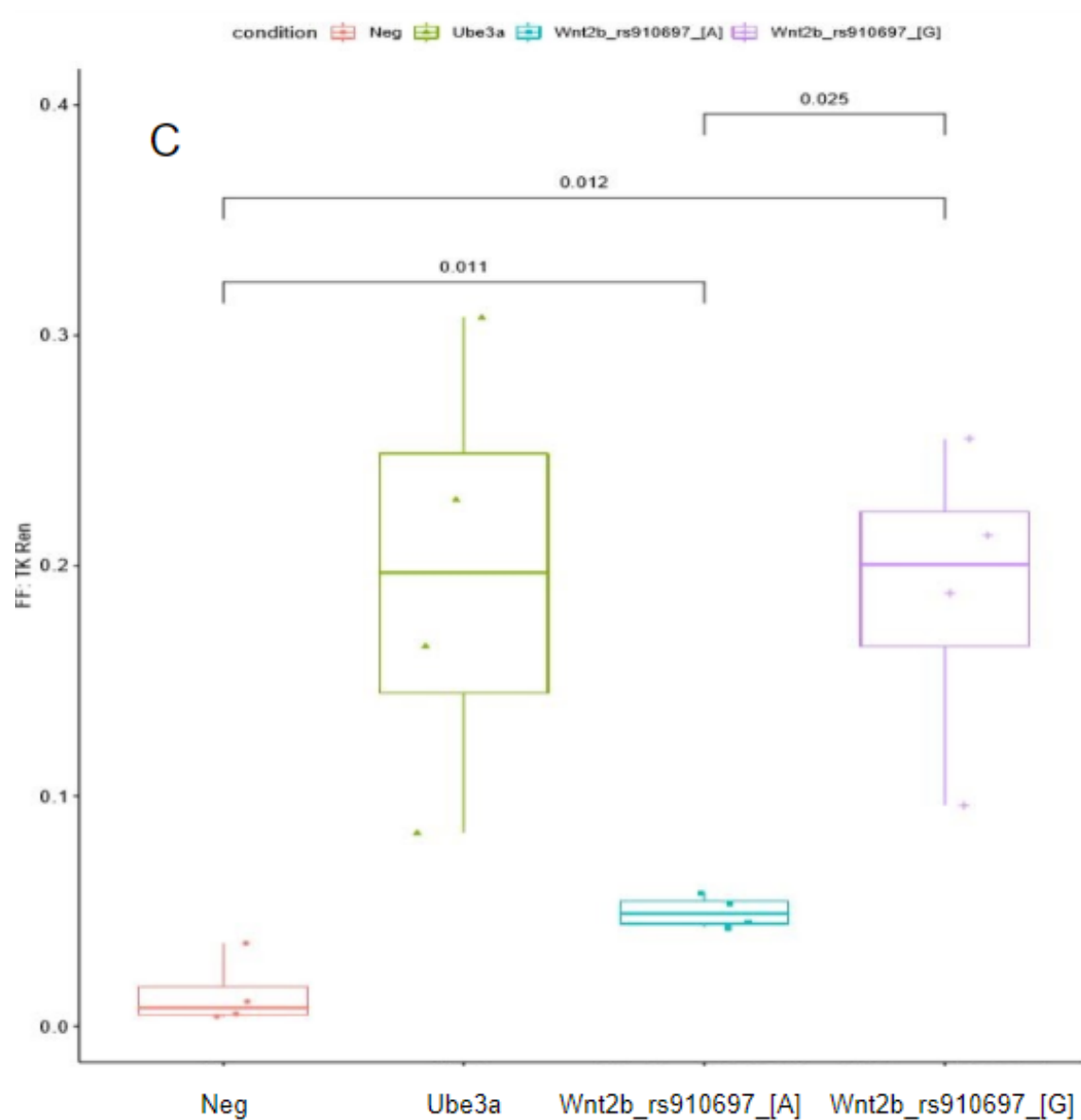
Wnt activation is significantly higher with SA-decreasing allele in HEK293 cells

Wnt signaling activation influences the proliferation of HEK293 cell lines (Jia, 2008). To find out whether there was differential activation of the Wnt signaling pathway in HEK293 cells containing the cortical surface area-increasing allele or the surface area-decreasing allele of *WNT2B*, HEK293 cells plated into 96-well plates were transiently transfected with the gene variants in question, or a positive or negative control. Each condition contained four replicates. The transfected cells were then lysed and activation levels of the Wnt pathway were obtained through a luciferase assay analyzing the activation of Beta-catenin compared to a nonspecific Renilla control. Successful transient transfection of HEK293 cells with an observed transfection efficiency greater than 50% (visualized onscope by GFP presence), followed by a luciferase assay to measure the activity of the canonical Wnt pathway, yielded a consistent trend in Wnt signaling activation with similar levels of statistical significance between conditions (Fig. 3, panels A-C). Cells transfected with the surface area-decreasing allele (WNT2B rs910697 [G]) showed a significant increase in Wnt activation when compared to the surface area-increasing allele (WNT2B rs910697 [A]). This is surprising, because Wnt activation is expected to lead to increased proliferation, which would ultimately increase surface area. P-values between the surface area-increasing and surface area-decreasing alleles within the reproducible data set ranged from 0.025 to 0.033 (Fig. 3, panels A-C). Statistical significance was calculated using a two-tailed t-test in Rstudio and verified using Microsoft Excel.

Fig 3. HEK293 Luciferase Data Summary







Summary of HEK293 luciferase data for three consecutive transfections (panels A, B, and C). X axis labels represent overexpression plasmid used for respective conditions. Each condition contains four replicates, denoted by colored dots in each

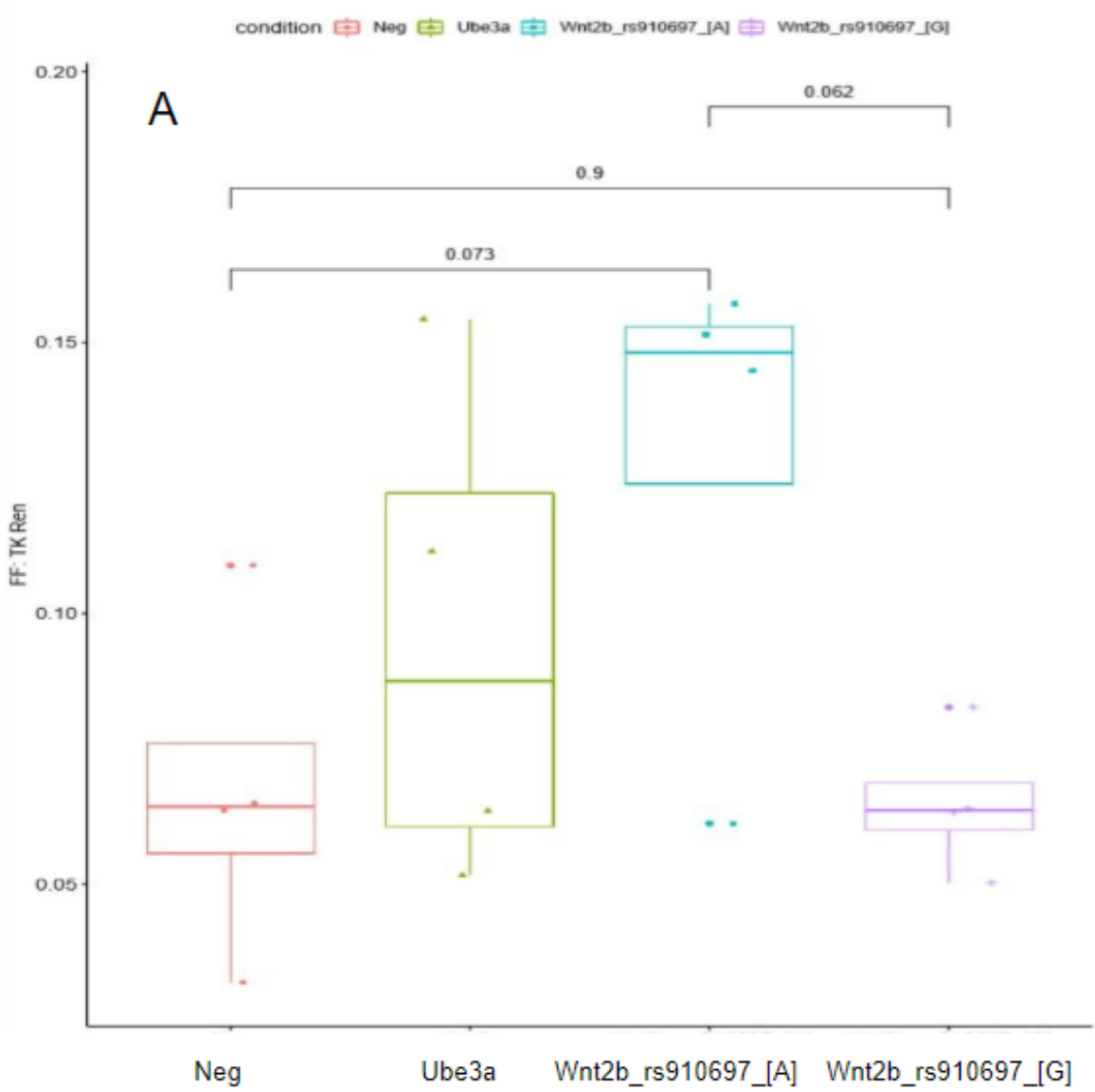
condition. X axis labels in all panels, from left to right: negative control (Neg), positive control (Ube3a), surface area-increasing *WNT2B* (Wnt2b_rs910697_[A]), surface area-decreasing *WNT2B* (Wnt2b_rs910697_[G]). Y axis represents the ratio between FF and TK Renilla, revealing the normalized Wnt activation level for each condition. P-value of Wnt activation difference between Wnt2b_rs910697_[G] and Wnt2b_rs910697_[A] is displayed above the last comparison bar in each graph.

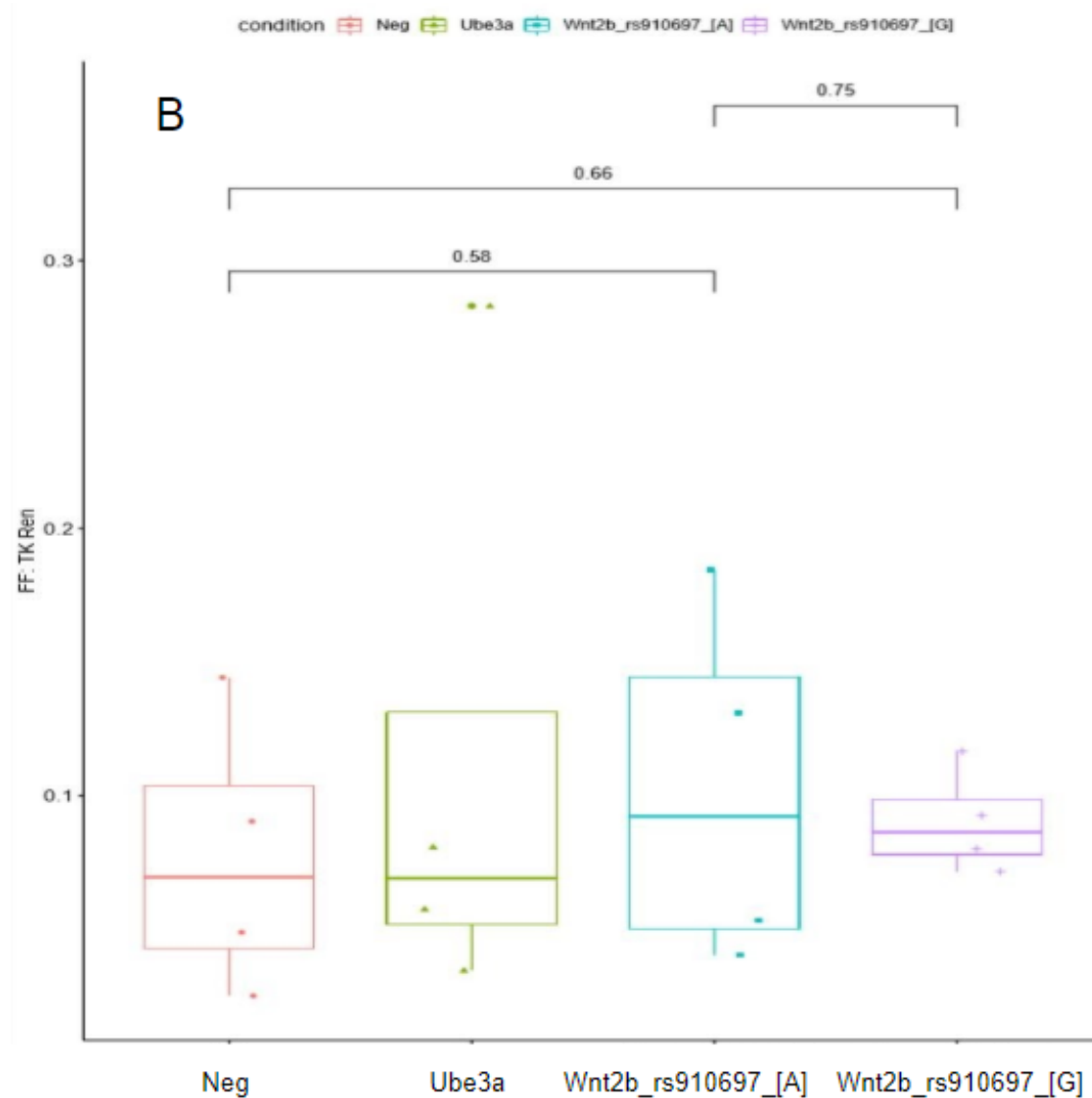
hNP Cells Exhibit Highly Variable and Irreproducible Wnt Activation Levels

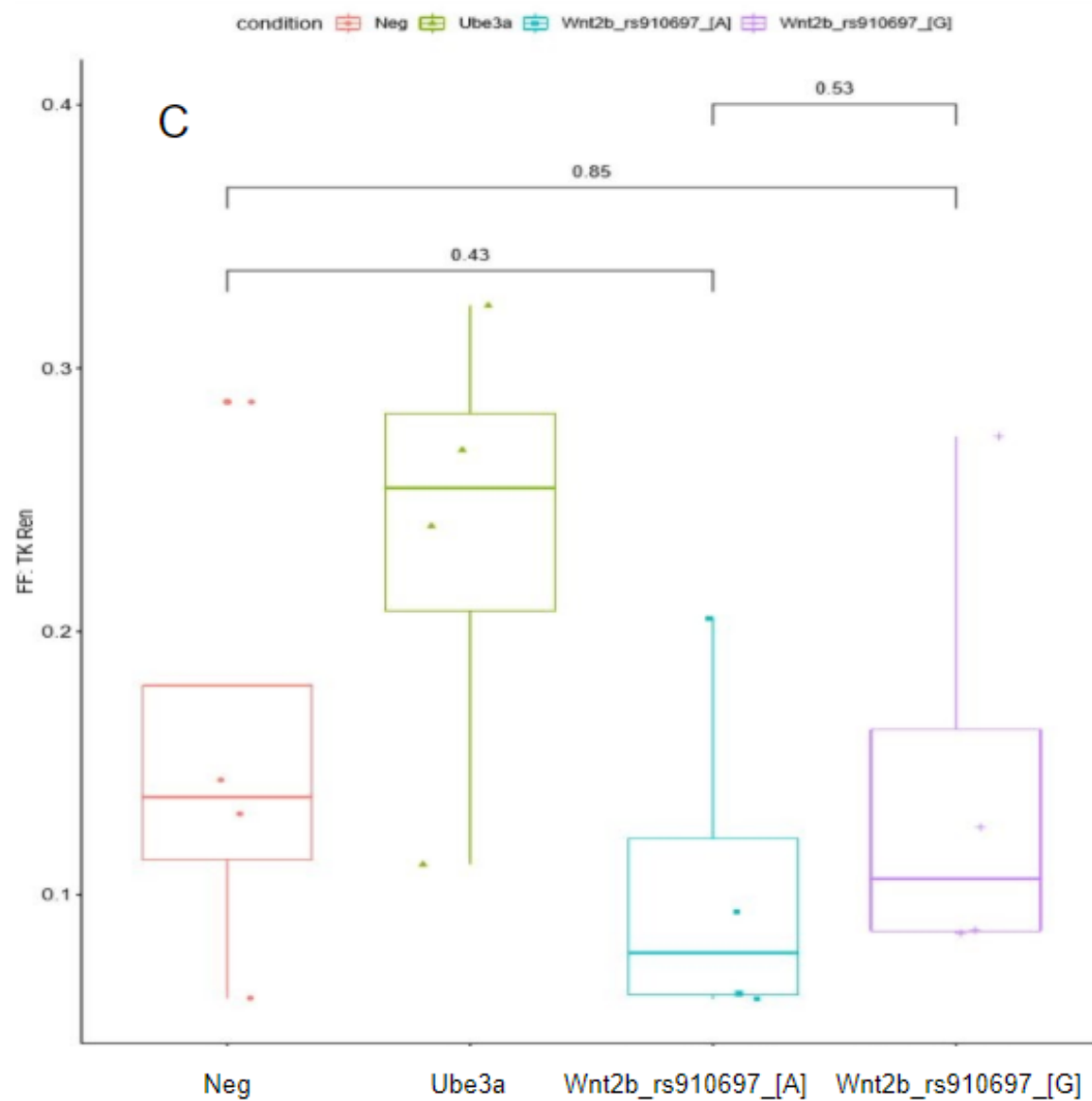
After identifying a significant and reproducible pattern of Wnt activation in HEK293 cells upon transient transfection, we sought to execute the same transfection process in hNP cells. The identification of Wnt activation patterns in hNP cells containing the surface area-increasing and surface area-decreasing alleles is necessary in evaluating how the variant in *WNT2B* may impact the proliferation dynamics of neural progenitor cells during cortical development. Neural progenitors are the cell type associated with proliferation during cortical development; their proliferation dynamics directly influence how the cortex is shaped. Prior literature examining the effect of Wnt signaling in cortical development (Chenn, 2008) has shown that increases in Wnt signaling generally increases proliferation. hNP cells plated into 96-well plates were transiently transfected with the gene variants in question, in addition to a positive and negative control (Ube3A and no overexpression plasmid, respectively). All cells plated were obtained from the same donor. The transfected cells were then lysed and activation levels of the Wnt pathway were obtained through a luciferase assay analyzing the activation of Beta-catenin compared to a nonspecific Renilla control. Successful transient transfection of hNP cells with an observed transfection efficiency greater than 35%, followed by a luciferase assay to

measure the activity of the canonical Wnt pathway, yielded an inconsistent trend in Wnt signaling activation with highly variable levels of statistical significance within and between conditions (Fig. 4, panels A-C). Concerningly, Wnt activation in the positive control condition (*UBE3A*) is inconsistently activated between transfections, with high variability within the condition. Cells transfected with the surface area-decreasing allele (WNT2B rs910697 [G]) showed no consistent increase or decrease in Wnt activation when compared to the surface area-increasing allele (WNT2B rs910697 [A]). In addition, the surface area-decreasing allele showed highly variable levels of Wnt activation between plates, as well as between wells within a single plate. The high variation within conditions as well as the inconsistent positive control activation of Wnt signaling indicates that these results are not trustworthy. Technical variables that could account for these inconsistencies are addressed in the next section. P-values between the reference and alternative alleles within the reproducible data set ranged from 0.062 to 0.75 (Fig. 4, panels A-C). Statistical significance was calculated using a two-tailed independent t-test in Rstudio and verified using Microsoft Excel.

Figure 4. hNP Luciferase Data Summary







Summary of hNP luciferase data from three consecutive transfections (panels A, B, and C).. X axis labels represent overexpression plasmid used for respective conditions. Each condition contains four replicates, denoted by colored dots corresponding to each condition. X axis labels in all panels, from left to right: negative control (Neg), positive control (Ube3a), surface area-increasing

WNT2B (Wnt2b_rs910697_[A]), surface area-decreasing *WNT2B* (Wnt2b_rs910697_[G]). Y axis represents the ratio between FF and TK Renilla, revealing the normalized Wnt activation level for each condition. P-value of Wnt activation difference between Wnt2b_rs910697_[G] and Wnt2b_rs910697_[A] is displayed above the last comparison bar in each graph.

Discussion

Multiple proteins in the Wnt family have been shown to influence the development of the human cortex through their impact on neural progenitor cell proliferation dynamics (Chenn, 2008). In HEK293 cells, a differential activation pattern in Wnt signaling was observed between the surface area-increasing and surface area-decreasing alleles of *WNT2B*. In hNP cells, the margin of difference between the surface area-increasing and surface area-decreasing alleles in Wnt activation was ultimately indeterminate due to the inconsistent actions of the positive control *UBE3A*. From these findings, it is difficult to make any conclusions about the variant of *WNT2B* having any effect on Wnt signaling activation in hNP cells. The data does not support the assumption that the variant has any direct causative impact on differences in cell proliferation dynamics induced by differential Wnt signaling levels in embryonic brain tissue. To definitively make this conclusion, however, a proliferation study would still need to be conducted in hNP cells containing the surface area-increasing and surface area-decreasing alleles, comparing them to a consistent and reliable positive control. A possible positive control candidate is *WNT3A*, which has been shown in previous literature to significantly activate Wnt signaling in neural tissue (Rao, 2019). In the same vein, it must be noted that the luciferase technology only detects

activation of the Wnt pathway by proxy, through activation by Beta-catenin. It does not measure any of the downstream steps of Wnt activation, such as how much of the Wnt target genes are ultimately expressed. Also important to note is the fact that the overall Wnt activation levels in the assays seemed to be dependent on the DNA prep from which the overexpression plasmids were harvested.

It is possible that transient whole-plasmid transfection is not the best method to use for DNA insertion in hNP cells. Transfection efficiency was estimated by GFP presence in transfected wells. It is entirely possible, and in fact quite likely based on the high variation within and between conditions, that not all of the plasmid constructs were able to enter the cells. If the BAR or Renilla constructs were not present in the cells, then the luciferase data would be inconsistent, and largely inaccurate. An alternative method, such as lentiviral transduction, would most likely be ideal for inserting all of the constructs simultaneously with high efficiency. If lentiviral transduction is completed with the conditions listed above, and reproducible results are yielded, we expect that the surface area-decreasing allele will show a significant decrease in Wnt activation compared to the surface area-increasing allele. A proliferation study would then be conducted, ideally showing a corresponding decrease in proliferation dynamics in human neural progenitor cells. This would in turn indicate that the common variant found in *WNT2B* could have an impact on human cortical surface area development. Such evidence could provide a potential target for future studies into genetic variants that impact risk for neuropsychiatric disorders such as autism spectrum disorder (ASD) and schizophrenia, since altered cortical

structure is highly associated with these conditions (Hoset, 2018; Kwan, 2016). After finding whether the variant has an effect on Wnt signaling activation and proliferation dynamics in hNP cells, the mechanism that causes this synonymous variant to have such an impact should be explored. Possible candidates for study include alterations to a nearby m6A DNA methylation site, tRNA abundance, and miRNA interference.

Overall, this research has provided evidence that the common genetic variant found in *WNT2B* shows differential activation of the Wnt signaling pathway in embryonic kidney tissue. Whether the variant impacts Wnt signaling in embryonic brain tissue remains unclear, but a solid framework for future experimentation has been laid for obtaining a concrete answer.

Acknowledgments

Thank you to everyone in the Stein and Zylka labs, especially Jason Stein, Justin Wolter, Brandon Le, Jordan Valone, Mike Lafferty, and Oleh Krupa. All of the advice, guidance, and sympathetic gnashing of teeth are what made all of this research possible. Also, thank you to Amy Maddox, my thesis advisor, for all of the tips on compiling my research into a comprehensive thesis.

References

Grasby, Katrina L. (2014). *The Genetic Architecture of the Human Cerebral Cortex*.

BioRxiv.org. Available at: <https://www.biorxiv.org/content/10.1101/399402v3.article-info>

Wiese, K., van Amerongen, R. and Nusse, R. (2018). *Wnt signalling: conquering complexity*.

[online] Web.stanford.edu. Available at:

http://web.stanford.edu/group/nusselab/cgi-bin/wnt/sites/default/files/dev165902.full_.pdf

Nusse, R. (2019). *The Wnt Homepage*. [online] Web.stanford.edu. Available at:

<http://web.stanford.edu/group/nusselab/cgi-bin/wnt/>

Yi, J., Wolter, J., Zylka, M., Fragola, G., Paranjape, S., Walker, M., Choudhury, R., Emanuele,

M. and Major, M. (2017). *The autism-linked UBE3A T485A mutant E3 ubiquitin ligase activates the Wnt/ β -catenin pathway by inhibiting the proteasome*. [online] Available at:

<https://www.ncbi.nlm.nih.gov/pubmed/28559284>

Rao, D., Ferguson, R., Bordeaux, E., Yamamoto, T., Bitler, B. and Sikora, M. (2019). *WNT4 and WNT3A activate cell autonomous Wnt signaling independent of PORCN and secretion*. [online] biorxiv.org. Available at: <https://www.biorxiv.org/content/10.1101/333906v3.full>

Biechele T.L., Moon R.T. (2008) *Assaying β -Catenin/TCF Transcription with β -Catenin/TCF Transcription-Based Reporter Constructs*. In: Vincan E. (eds) *Wnt Signaling*. Methods in Molecular Biology™, vol 468. Humana Press

Wang, X., Lu, Z., Gomez, A., Hon, G., Yue, Y., Han, D., Fu, Y., Parisien, M., Dai, Q., Jia, G., Ren, B., Pan, T. and He, C. (2014). *N6-methyladenosine-dependent regulation of messenger RNA stability*. [online] Available at: <https://www.ncbi.nlm.nih.gov/pmc/articles/PMC3877715/>

Sethi, J. and Vidal-Puig, A. (2008). *Wnt signalling at the crossroads of nutritional regulation*. [online] Available at: <https://www.ncbi.nlm.nih.gov/pmc/articles/PMC4303997/>

Addgene.org. (2019). *Addgene: pcDNA-Wnt2B2*. [online] Available at: <https://www.addgene.org/35907/>

P, R. (2000). *Radial unit hypothesis of neocortical expansion*. - PubMed - NCBI. [online]

Ncbi.nlm.nih.gov. Available at: <https://www.ncbi.nlm.nih.gov/pubmed/10929315>

Chenn, A. (2008). *Wnt/ β -catenin signaling in cerebral cortical development*. [online] PubMed

Central (PMC). Available at: <https://www.ncbi.nlm.nih.gov/pmc/articles/PMC2634251/>

Pääbo, S. (2014). *The Human Condition-A Molecular Approach*. Cell [online] 157(1),

pp.216-226. Available at:

[https://www.cell.com/cell/fulltext/S0092-8674\(13\)01605-X?_returnURL=https%3A%2F%2Flinkinghub.elsevier.com%2Fretrieve%2Fpii%2FS009286741301605X%3Fshowall%3Dtrue](https://www.cell.com/cell/fulltext/S0092-8674(13)01605-X?_returnURL=https%3A%2F%2Flinkinghub.elsevier.com%2Fretrieve%2Fpii%2FS009286741301605X%3Fshowall%3Dtrue)

Kwan, V., Unda, B. K., & Singh, K. K. (2016). *Wnt signaling networks in autism spectrum disorder and intellectual disability*. Journal of neurodevelopmental disorders, 8, 45.

doi:10.1186/s11689-016-9176-3

Hoseth, E., Krull, F., Dieset, I., Mørch, R., Hope, S., Gardsjord, E., Steen, N., Melle, I.,

Brattbakk, H., Steen, V., Aukrust, P., Djurovic, S., Andreassen, O. and Ueland, T. (2018).

Exploring the Wnt signaling pathway in schizophrenia and bipolar disorder. Translational

Psychiatry, [online] 8(1). Available at:

<https://www.nature.com/articles/s41398-018-0102-1#rightslink>

Jia, L., Miao, C., Cao, Y., Duah, EK. (2008). *Effects of Wnt proteins on cell proliferation and apoptosis in HEK293 cells*. Cell Biology International. Available at:

<https://www.ncbi.nlm.nih.gov/pubmed/18462958>